Supplementary Figure 1

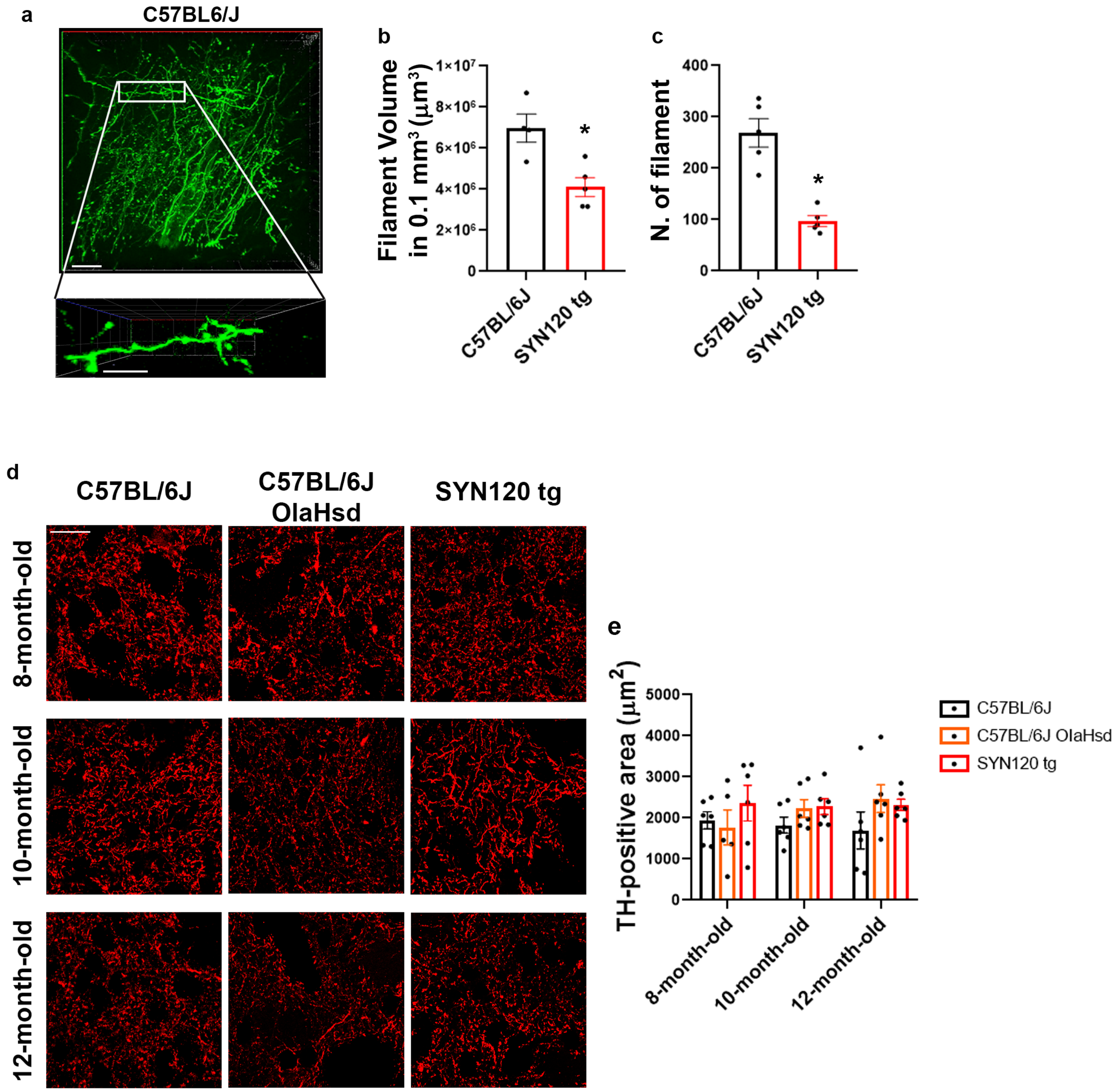

Supplementary Figure 2

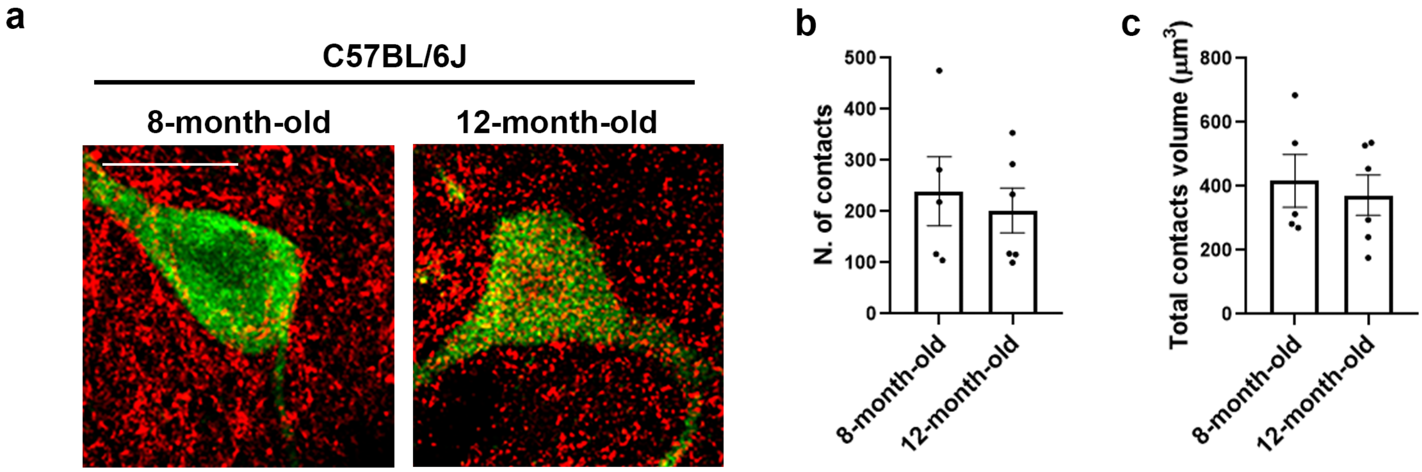

Supplementary Figure 3

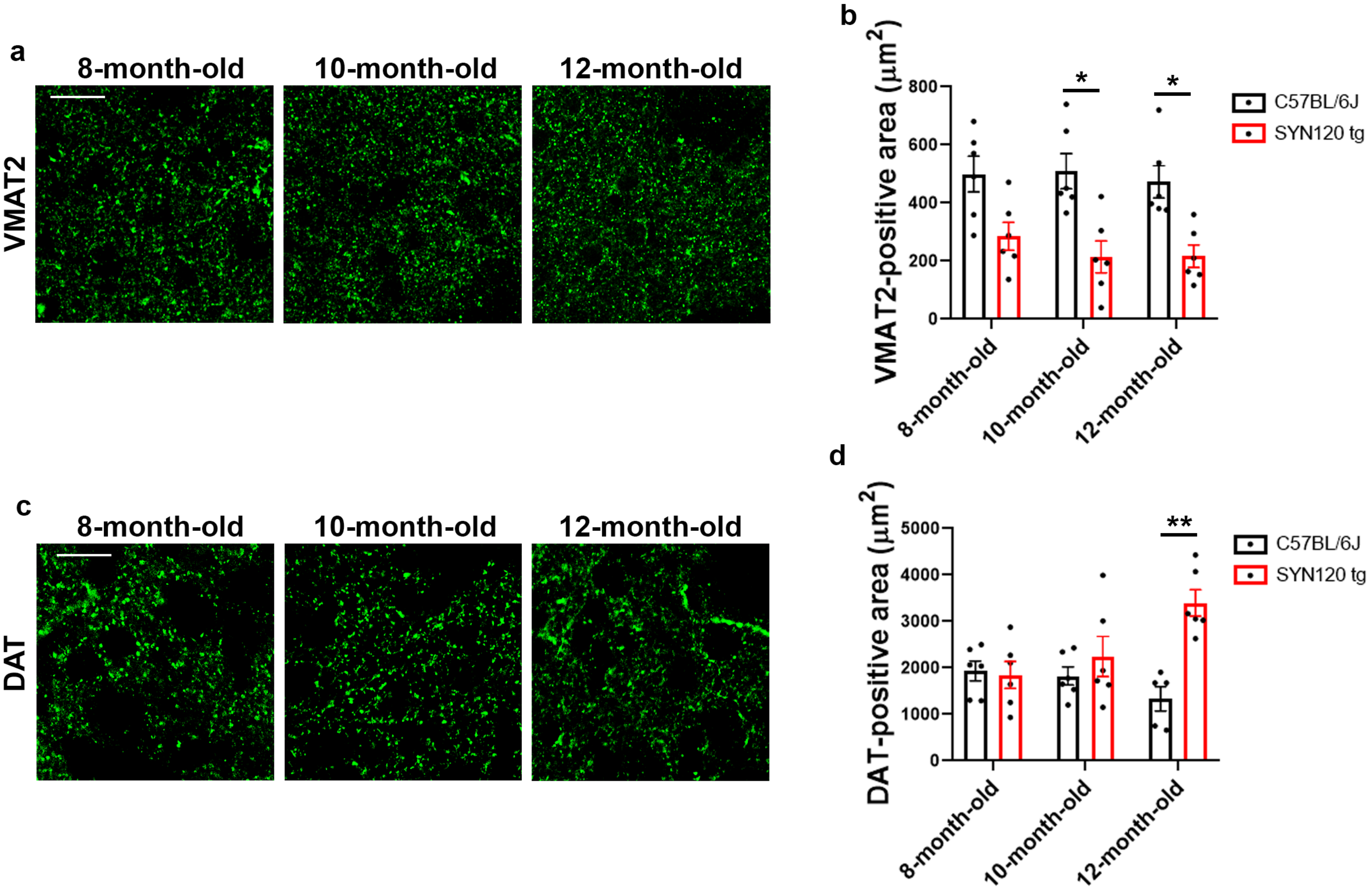

Supplementary Figure 4

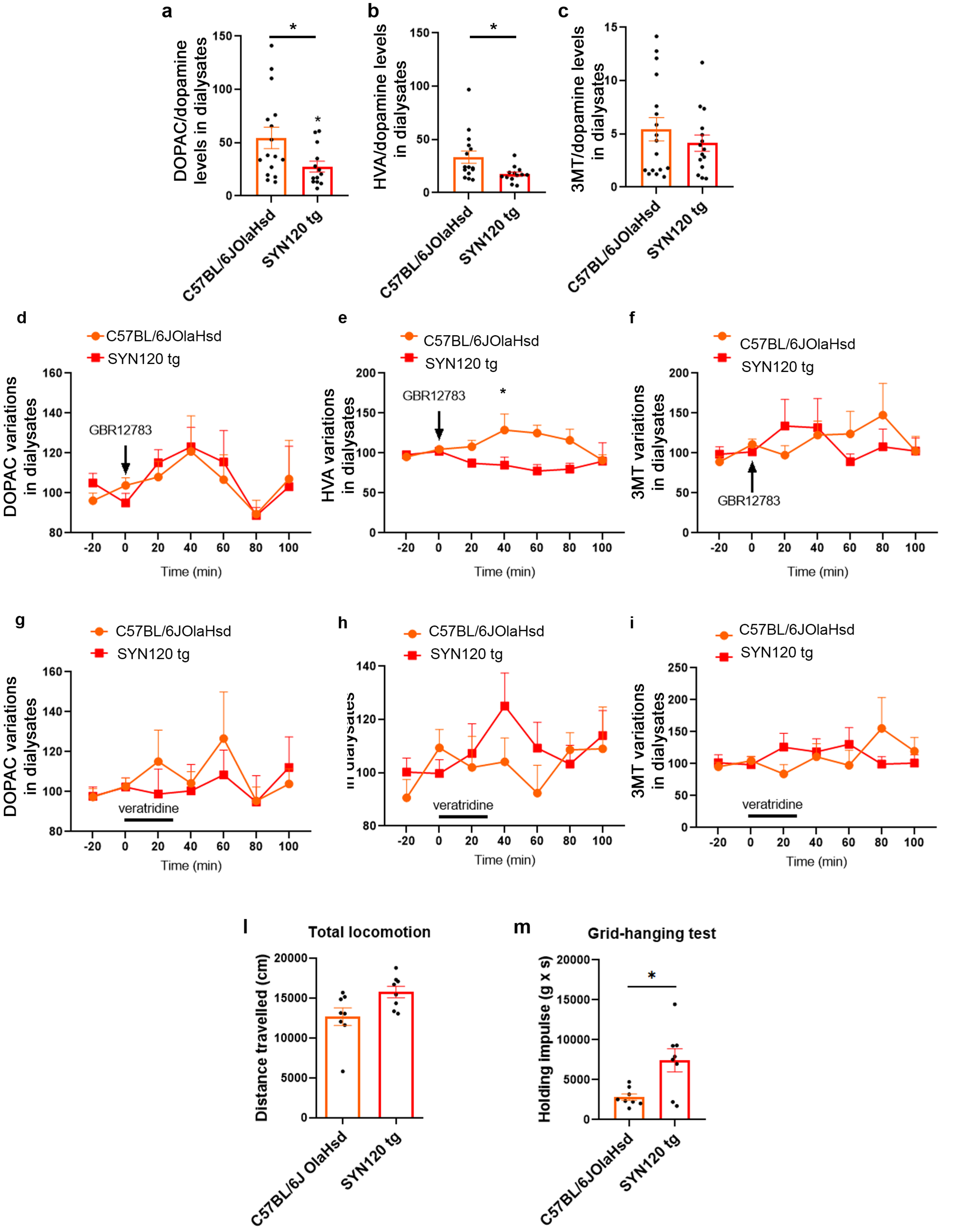

Supplementary Figure 5

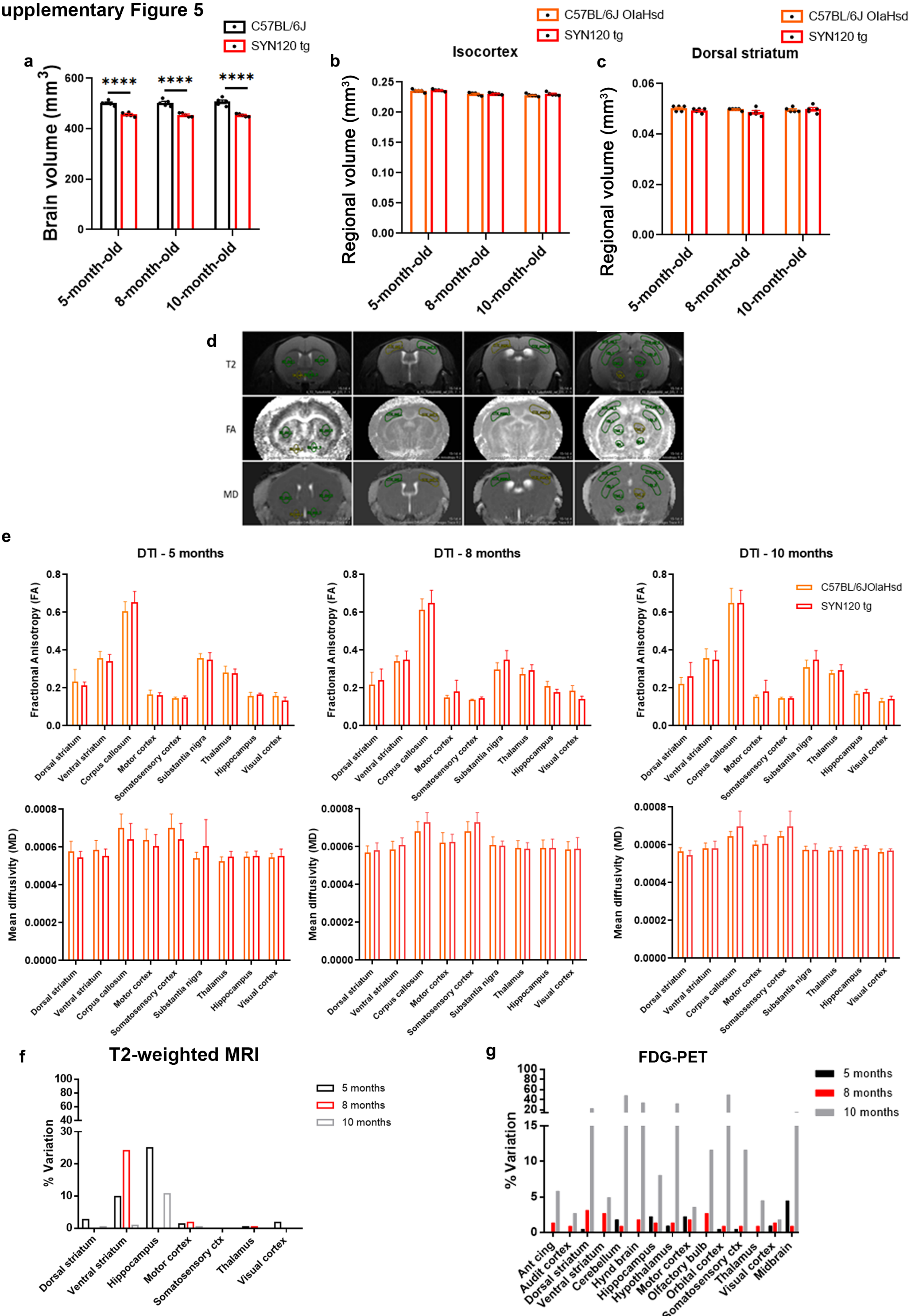

Supplementary Figure 6

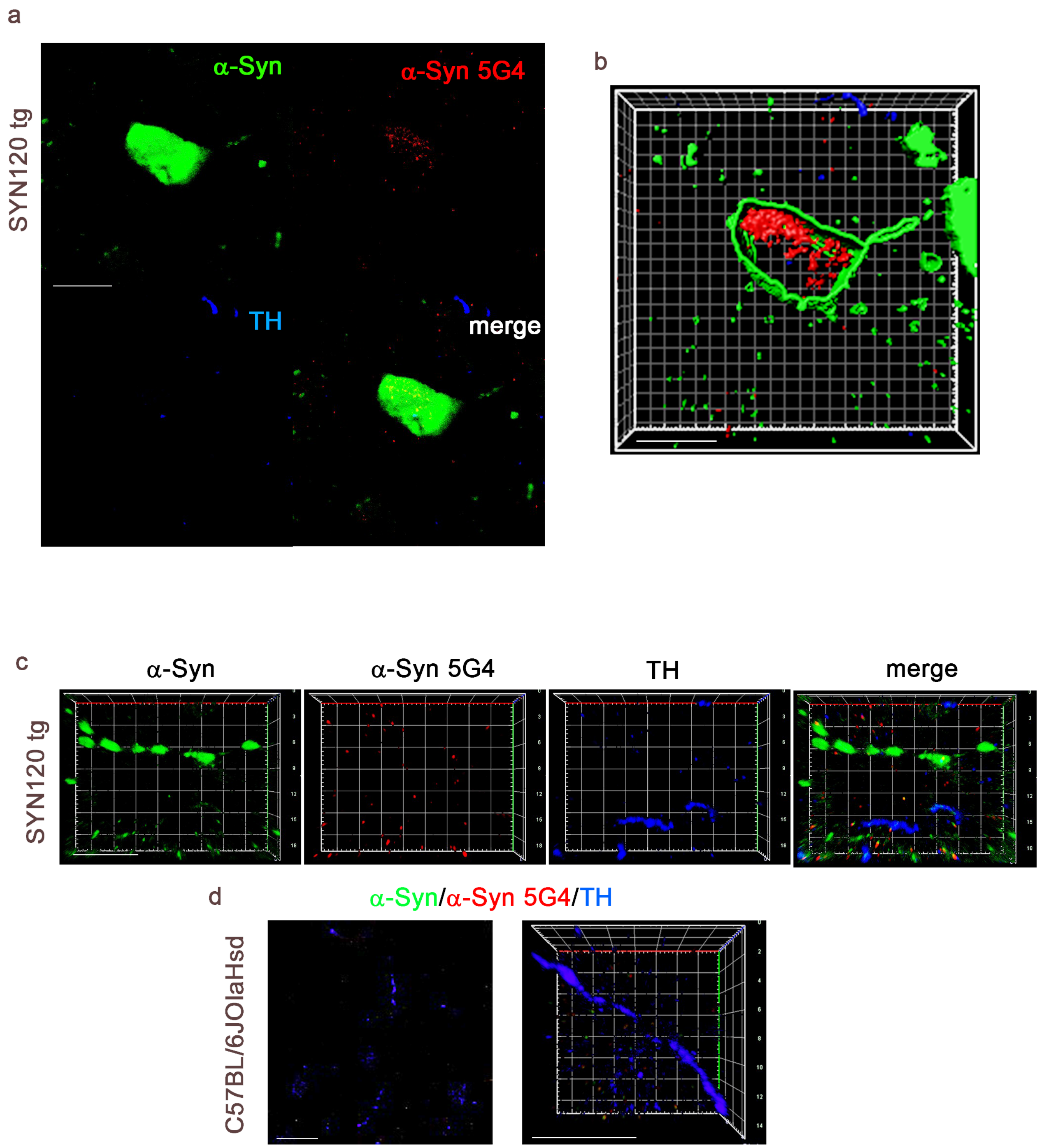

Supplementary Fig. 1 Striatal GFP-positive fibres two-photon-based 3D reconstruction in 12 month-old C57BL/6J mice. a. Representative 3D reconstruction of z-stack imaging of GFP-positive fibres in the striatum of C57BL/6J mice. Scale bar = 50 µm, higher magnification panel = 20 µm. b. Graph is showing a significant decrease in the total volume of GFP-positive fibres in the dorsal striatum of SYN120 tg mice when compared to C57BL/6J animals. * $p < 0.05$, non-parametric Mann-Whitney two-tailed test. N = 5 mice each group. c. Graph is showing a significant reduction in the number of GFP-positive striatal fibres in SYN120 tg mice when compared to C57BL/6J animals. * $p < 0.05$, non-parametric Mann-Whitney two-tailed test. N = 5 mice each group. d. Representative images showing TH-immunolabelling in the striatum of C57BL/6J, C57BL/6JOlaHsd and SYN120 tg mice at 8, 10 and 12 months of age. Scale bar = 20 µm. e. Graph is showing the analysis of TH-positive area in the striatum of C57BL/6J, C57BL/6JOlaHsd and SYN120 tg mice at 8, 10 and 12 months of age. No differences were detected between the total area of TH-positive fibres of the three mouse lines analysed. Two-way ANOVA + Bonferroni multiple comparisons test. N = 6 mice each group.

Supplementary Fig. 2 Analysis of striatal contacts between ChAT-positive neurons and TH-positive fibres in C57BL/6J control mice. a. Representative images showing ChAT (green) and TH (red) immunolabelling in C57BL/6J at 8 and 12 months of age. Scale bar = 10 µm. b. Graph is showing the number of contacts between ChAT-positive neurons and TH-positive fibres in C57BL/6J animals at 8 and 12 months of age. No differences were detected between 8-month-old and 12-month-old animals. Mann-Whitney two-tailed test. N = 5/6 mice each group. c. Graph is showing the analysis of the ChAT/TH contact volume in 8- and 12-month-old control mice. No differences were detected neither at 8 or 12 months of age. Mann-Whitney two-tailed test. N = 5/6 mice each group.

Supplementary Fig. 3 Striatal VMAT2 and DAT immunofluorescence in 8-, 10- and 12-month-old C57BL/6J mice. a. Representative images showing VMAT2 immunostaining in the striatum of C57BL/6J mice. Scale bar = 20 µm. b. Graph is showing the analysis of VMAT2-positive area, expressed in μm^2, in the striatum of C57BL/6J and SYN120 tg mice at 8, 10 and 12 months of age. Please note the statistically significant decrease of VMAT2-positive area in the striatum of SYN120 tg mice at 8, 10 and 12 months of age when compared to C57BL/6J littermates. * $p < 0.05$. Two-way ANOVA + Bonferroni multiple comparisons test. N = 6 mice each group. c. Representative images showing DAT immunolabelling in C57BL/6J mice. Scale bar = 20 µm. d. Graph is showing the analysis of DAT-immunopositive area, expressed in μm^2, in the striatum of C57BL/6J and SYN120 tg mice at 8, 10 and 12 months of age. Please note the statistically significant increase of DAT-positive area in the striatum of SYN120 tg mice at 12 months of age when compared to C57BL/6J littermates. ** $p < 0.01$. Two-way ANOVA + Bonferroni multiple comparisons test. N = 6 mice each group.

Supplementary Fig. 4 Analysis of striatal dopamine turnover. a. Graph is showing that ratio between the extracellular levels of DOPAC and dopamine were significantly reduced in SYN120 tg mice when compared to C57BL/6JOlaHsd animals. N = 15/17 measurements. * $p < 0.05$, non-parametric Mann-Whitney two-tailed test. b. Graph showing that the ratio between the extracellular levels of HVA and dopamine were significantly decreased in SYN120 tg mice when compared to C57BL/6J animals. N = 15/17 measurements. * $p < 0.05$, non-parametric Mann-Whitney two-tailed test. c. Graph is showing the ratio between the extracellular levels of 3MT and dopamine. No differences were detected between SYN120 tg and C57BL/6JOlaHsd mice. N = 15/17 measurements. Non-parametric Mann-Whitney two-tailed test. d-f. Acute effect of systemic GBR12783 (20 mg/kg; i.p.) administration on extracellular dopamine metabolites DOPAC (e), HVA (e) and 3MT (f) in SYN120 tg and C57BL/6JOlaHsd mice. Dialysate levels of dopamine metabolites, expressed as percentages of baseline, show differences in C57BL/6JOlaHsd mice only for HVA 40 and 60 minutes after GBR12783 administration vs basal values (both -20 and 0 time-points). * $p < 0.05$. One-way ANOVA + Bonferroni multiple comparisons test. N = 8/9 mice each group. g-i. Reverse dialysis of veratridine (10 µM; for 30 minutes) in the striatum on the striatal extracellular levels of dopamine metabolites DOPAC (g), HVA (h) and 3MT (i) of SYN120 tg and C67BL/6JOlaHsd mice. Dialysate levels of dopamine metabolites, expressed as percentages of baseline, did not show changes after veratridine administration. One-way ANOVA + Bonferroni multiple comparisons test. N = 7/8 mice each group. l. Analysis of the distance travelled of SYN120 tg and C57BL/6JOlaHsd animals in the Open field test at 10 months of age did not evidence differences between SYN120 tg and C57BL/6JOlaHsd mice. Non-parametric Mann-Whitney two-tailed test. N = 8/9 mice each group. m. Ten-month-old SYN120 tg animals exhibited increased holding impulse in grid hanging test vs C57BL/6JOlaHsd littermates. * $p < 0.05$, non-parametric Mann-Whitney two-tailed test. N = 8/9 mice each group.

Supplementary Fig. 5 MRI-based brain volume, FA, MD analysis and radiomic studies of T2-weighted MRI and [^{18}F]-FDG PET-CT. a. Total brain volume measured on T2-weighted images in 5-, 8- and 10-month-old SYN120 tg and C57BL/6J animals. **** $p < 0.0001$, two-way ANOVA + Bonferroni multiple comparisons test. b, c. Regional brain volume measured on T2-weighted images in 5-, 8- and 10-month-old SYN120 tg and C57BL/6JOlaHsd animals did not show differences in the isocortex (b) and dorsal striatum (c) between strains. Two-way ANOVA + Bonferroni multiple comparisons test. N = 5 mice. d. Image showing the representative regions of interest (ROIs) considered for the segmentation of region identification for FA and MD. e. DTI-MRI analysis of FA and MD of SYN120 tg and C57BL/6JOlaHsd animals at 5, 8 and 10 months of age. f. Radiomic analysis of T2-weighted MRI in which data are expressed as % of Variation of SYN120 tg and C57BL/6JOlaHsd animals at 5, 8 and 10 months of age. g. Radiomic analysis of striatal uptake of [^{18}F]-FDG PET-CT images showing the % of Variation of SYN120 tg mice vs C57BL/6JOlaHsd littermates at 5, 8 and 10 months of age.

Supplementary Fig. 6 Diffusion and accumulation of α-Syn aggregates in the motor cortex of 8-month-old SYN120 tg mice. a. Representative images showing α-Syn-positive cells containing 5G4-labelled α-Syn aggregates in proximity to TH-positive filaments (in blue) in the motor cortex of 8 month-old SYN120 tg mice. Scale bar = 10 μm. b. Surface reconstruction of 3D z-stack images in panel a. Scale bar = 8 μm. c. Representative images showing an α-Syn-positive filament positive for 5G4-immunopositive aggregated α-Syn in proximity to TH-positive terminal in the motor cortex of 8 month-old SYN120 mice. Scale bar = 10 μm. d. Representative images showing the absence of α-Syn and 5G4-labelled α-Syn aggregates in proximity to TH-positive filaments in the motor cortex of C57BL/6JOlaHsd at 8 months of age.

Supplementary video 1 3D rendering of two-photon-based imaging of GFP-positive striatal fibres from C57BL/6JOlaHsd thick clarified sections.

Supplementary video 2 3D rendering of two-photon-based imaging of GFP-positive striatal fibres from SYN120 tg mice.

Supplementary video 3 3D rendering of two-photon-based imaging of GFP-positive striatal fibres from C57BL/6J mice.